



OPEN ACCESS

EDITED BY

Zhenwei Dai,
China Geological Survey (Geosciences
Innovation Center of Central South
China), China

REVIEWED BY

Ong Yang,
China University of Geosciences Wuhan,
China
Longwei Yang,
China Coal Technology Engineering Group,
China

*CORRESPONDENCE

Yong-hong Zeng,
✉ sdxpit@gmail.com

RECEIVED 02 January 2024

ACCEPTED 14 February 2024

PUBLISHED 04 March 2024

CITATION

Hu C, Zeng Y-h and Yao H-y (2024), Stability
analysis of slopes with cracks using the finite
element limit analysis method.
Front. Earth Sci. 12:1364347.
doi: 10.3389/feart.2024.1364347

COPYRIGHT

© 2024 Hu, Zeng and Yao. This is an
open-access article distributed under the
terms of the [Creative Commons Attribution
License \(CC BY\)](https://creativecommons.org/licenses/by/4.0/). The use, distribution or
reproduction in other forums is permitted,
provided the original author(s) and the
copyright owner(s) are credited and that the
original publication in this journal is cited, in
accordance with accepted academic practice.
No use, distribution or reproduction is
permitted which does not comply with
these terms.

Stability analysis of slopes with cracks using the finite element limit analysis method

Chao Hu, Yong-hong Zeng* and Hao-yu Yao

China Railway Eryuan Engineering Group Co., Ltd., Chengdu, China

There are numerous slope projects involved in railway and highway constructions, and ensuring the stability of slopes, especially those with cracks, is very important. Compared with the limit equilibrium method, the limit analysis method takes into account the soil's stress-strain behavior and boundary conditions, thereby yielding more rigorous and accurate results. The stability of slopes with cracks was examined using the finite element limit analysis method in this study. Results indicate that the stability of the slope decreases with the crack length, especially for slope with small slope ratio (i.e., $\alpha \leq 1:1.5$) and when l_c/H exceeds 25%. The influence of crack inclination angle on slope stability increases with crack length, and the safety factor is larger in cases of negative inclination value cases as compared to those in positive inclination value cases when $l_c/H \geq 0.33$. Values of safety factor are larger in cases of slope with reinforcement as compared to those without reinforcement, and the values of F increase by about 20%. Additionally, the slip planes for slopes with reinforcement are located 10% further away from the slope surface compared to those without reinforcement, and reinforcements enhance the slope integrity.

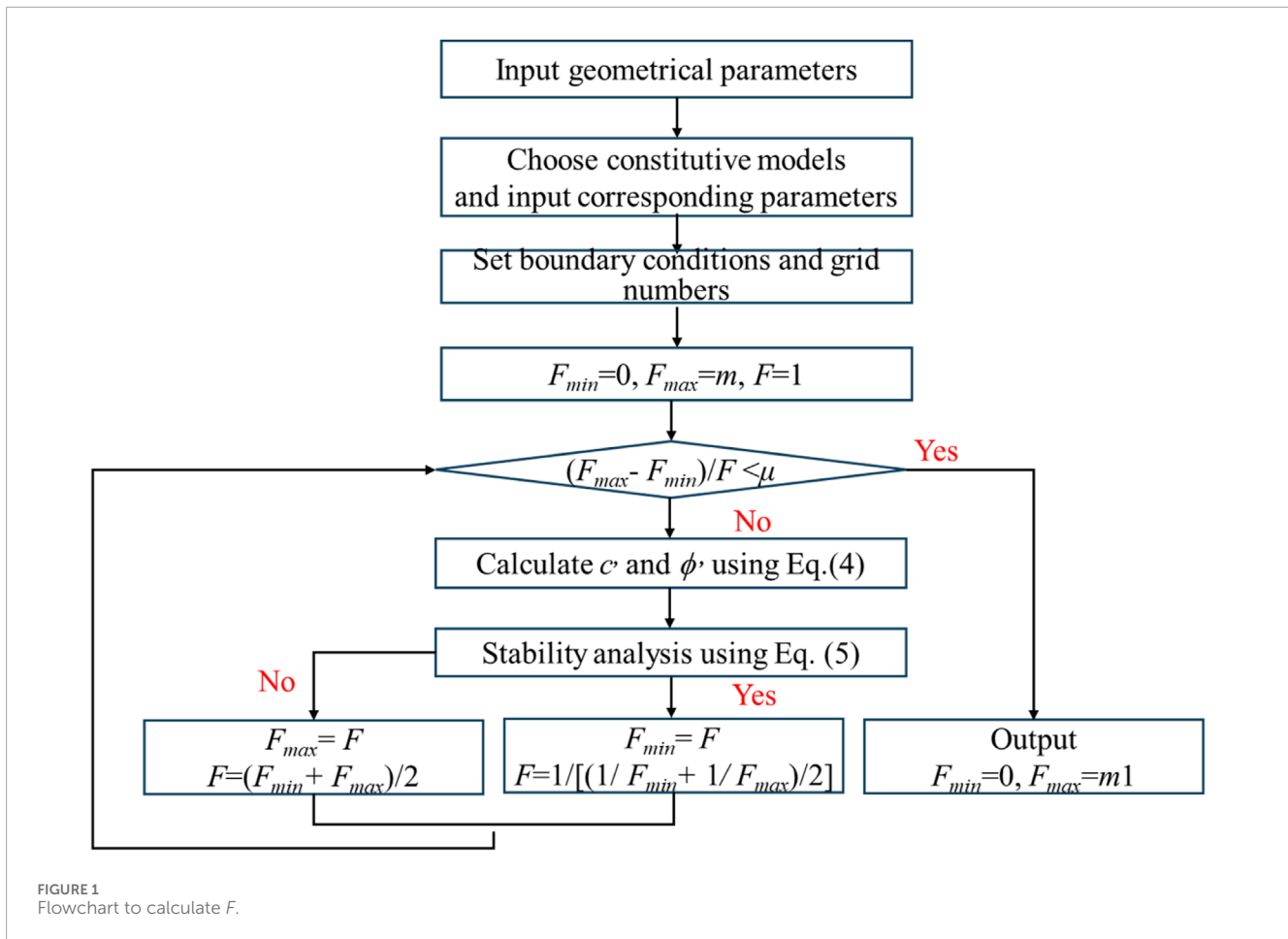
KEYWORDS

slope, crack, limit analysis, stability, reinforcement

1 Introduction

Numerous slope projects have been currently encountered in railway and highway constructions. Meanwhile, researchers have conducted many meaningful research on slope stability. For instance, [Zhang \(2022\)](#) conducted an assessment of rainfall erosion on embankment slopes in desert areas, and they also designed corresponding monitoring plans to monitor the displacement of the slope. [Dick et al. \(2015\)](#) reported an early-warning time-of-failure method to help analyze the stability and performance of open-pit mine slopes.

Numerous experimental researches have been carried out to investigate the performance of slopes with cracks. [Zhang et al. \(2009\)](#) conducted centrifuge model tests on slopes and utilized an image analysis system to measure slope deformation during loading. They found that tensional cracks occurring at the top of the slope led to localized strain and reduced slope stability. [Lin et al. \(2015\)](#) reported tilting platform model test results on Jinping dam. They found that the stability of the model decreased with the number of cracks, and cracks mainly formed along faults and propagated along structural weak planes. [Mehrijardi et al. \(2016\)](#) conducted a series of reduced scale model tests to investigate the bearing capacity of slopes under footing load. They observed cracks around the loading plate during the tests, and they also concluded that reinforcements could improve slope performance. [Zhou et al. \(2020\)](#) reported large-scale model tests results on the progressive failure of cracked slopes



subjected to rainfall. They found that the preferential flow in the cracks had a significant influence on the instability of slopes. [Yin et al. \(2023\)](#) conducted a comprehensive model test using a tilting platform to examine the characteristics of slope failure. They categorized the slope failure process into three stages. The first stage entailed a deformation phase characterized by scattered local cracks. This was followed by a destabilization stage marked by primary cracks. Finally, the retrogressive failure stage occurred, characterized by a proliferation of secondary crack.

Numerical methods are a more convenient and economic way as compared to the experimental methods above. [Chen et al. \(2014\)](#) reported results on the stability of expansive soil slopes using different limit equilibrium methods. They found that the generation of cracks significantly affected the stability of the slopes, especially when the influence of water was considered. [Mukhlisin and Khiyon \(2018\)](#) investigated the crack location, size, and depth on slope stability using GEO STUDIO 2007 software. They found that safety factors decrease sharply when cracks were located adjacent to the slope crest. [Jamalinia et al. \(2020\)](#) investigated the influence of evaporation on cracked slopes using a finite element method. They found that the presence of cracks could affect the water flux into the slope, which reduced the shear strength and the slope safety factor. [Stockton et al. \(2019\)](#) proposed a limit equilibrium method to analyze the influence of cracks on slope stability, where the cohesion and friction anisotropy were both considered. They concluded that

the shearing strength anisotropy had a significant influence on the tension crack formation and slope stability. They also found that in the case of anisotropic conditions with a horizontally weak plane, the slope failure surface tended to become elongated in the horizontal direction, resulting in a decrease of the tension crack depth. [Sari et al. \(2023\)](#) investigated the influence of drainage PVC pipe installed lengthwise into the slope on cracked slope using coupled programs SEEP/W and SLOPE/W. They concluded that the use of PVC pipe could increase the safety factor up to 7.7% for cracked slopes with weak layers.

Among the various numerical methods discussed above, the limit equilibrium method is more popular for designer as compared to numerical simulation methods, and it is recommended in most current specifications. However, the constitutive behavior of soil and boundary conditions can not be considered in this method. In recent years, the limit analysis method has been used in geotechnical engineering ([Krabbenhoft et al., 2015](#); [Jamalinia et al., 2020](#); [Xu et al., 2020](#); [Gao et al., 2021](#)). Unlike the limit equilibrium method, the stress - strain relationship can be considered, resulting in a more accurate and rigorous solution ([Sloan, 2013](#)). However, to the authors' best knowledge, the application of this method to cracked slopes is rarely reported in academic literatures.

In summary, cracks have a significant influence on slope stability. However, there is still limited research on numerical analysis of slopes with cracks, especially using the limit analysis method.

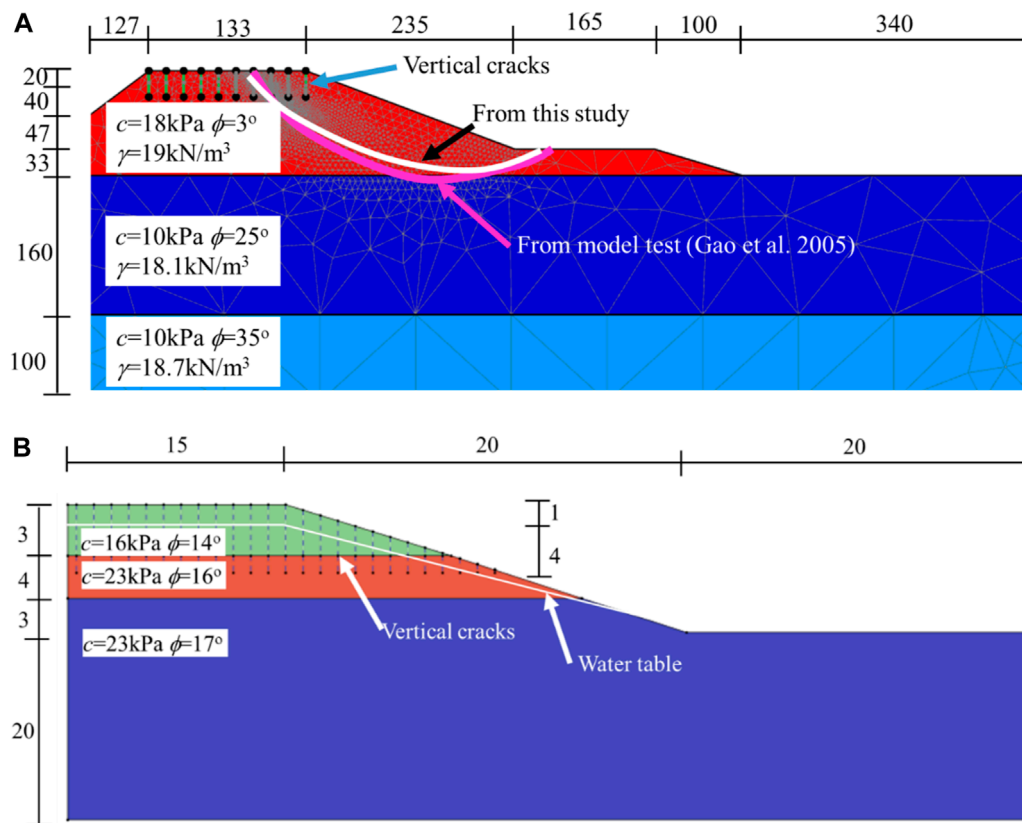


FIGURE 2 (A) Comparison of the slip planes from different method (Unit: m); (B) Schematic diagram of the slope model with cracks (Chen et al., 2014; unit: m).

Therefore, this study utilizes the finite element limit analysis method to investigate the stability of slopes with cracks, and then analyze the influences of crack length, inclination angle, strength, and reinforcement on slope stability and the shape of the failure surface. The results could help to enhance the comprehension of the stability of slope with cracks.

2 Limit analysis method

2.1 Upper bound theorem

Limit analysis can be classified into two categories: upper bound analysis and lower bound analysis. The former is particularly effective in analyzing the failure mechanism of slopes (Sloan, 2013). According to the upper bound theorem, the limit load, which is the minimum value among all the loads corresponding to admissible velocity fields, can be mathematically expressed as Eq. 1:

$$\int_S T_i v_i dS + \int_V f_i v_i dV \geq \int_V \sigma_{ij}^* \epsilon_{ij}^* dV \quad (1)$$

where S and V are the surface area and volume region, respectively; T_i and f_i are surface forces and body forces, respectively; v_i is the admissible velocity corresponding to the failure mechanism; and σ_{ij} and ϵ_{ij} are stress and strain, respectively.

TABLE 1 Parameters of the slope with cracks used for comparison.

Elevation (m)	Cohesion strength (kPa)	Friction angle (°)
27~30	16	14
23~27	23	16
0~23	23	17

The yield criterion can be described using the Mohr-Coulomb model and considering non-flow criterion for soils, which can be expressed as Eqs 2, 3:

$$Y = |\sigma_1 - \sigma_3| + |\sigma_1 + \sigma_3| \sin \phi^* - 2c^* \cos \phi^* \quad (2)$$

$$\begin{aligned} \tan \phi^* &= \frac{\cos \phi \cos \psi}{1 - \sin \phi \sin \psi} \tan \phi \\ c^* &= \frac{\cos \phi \cos \psi}{1 - \sin \phi \sin \psi} c \end{aligned} \quad (3)$$

where Y is the yield function; σ_1 and σ_3 are the maximum and minimum stresses, respectively; ψ is the dilation angle; c and ϕ are the cohesion strength and friction angle, respectively; and c^* and

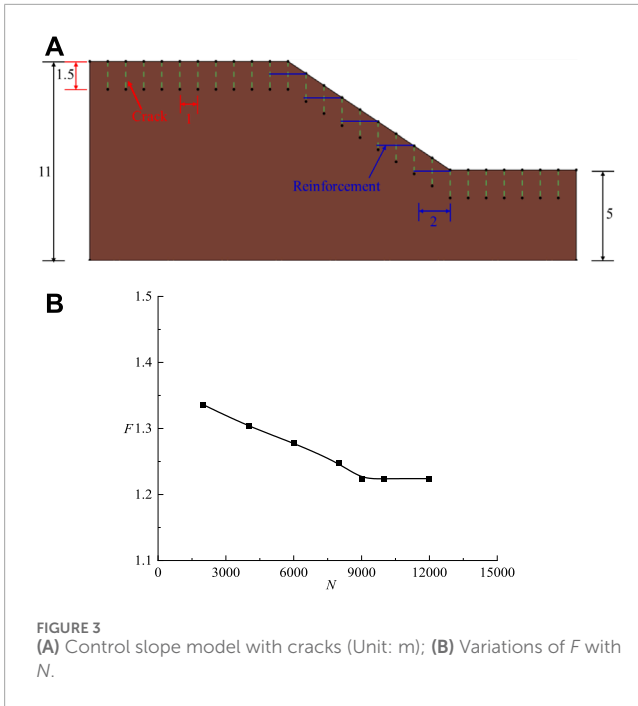


FIGURE 3 (A) Control slope model with cracks (Unit: m); (B) Variations of F with N .

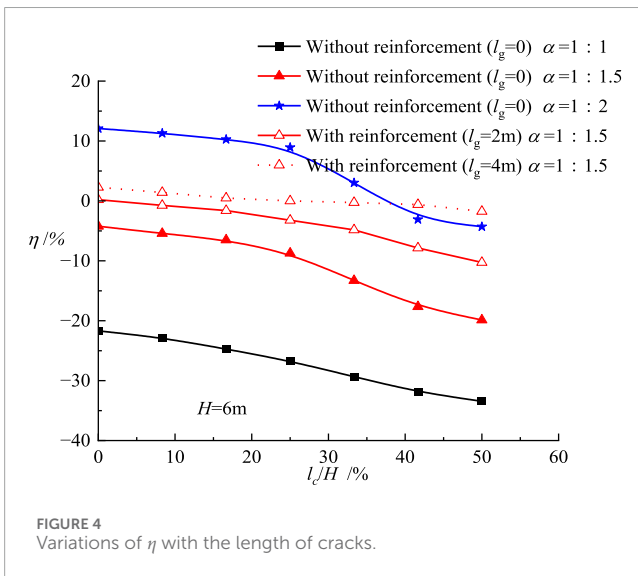


FIGURE 4 Variations of η with the length of cracks.

3 Parametric analysis

In section, parametric analysis was carried out to investigate the influence of crack length, crack inclination, and crack strength, respectively using the above validated finite element limit analysis method. The following control model shown in Figure 3A with parameters listed in Table 3 is used in this section. It should be noted that all the parameters are the same as those in Table 3 except that specified in the following analysis.

Many previous researches have corroborated the presence of cracks within slope except those near the slope surface. However, due to the irregular distribution of cracks within slopes and the challenge of quantitatively characterizing their distribution, current research predominantly focuses on vertical cracks near

TABLE 3 Parameters used in control model.

Parameter	Value
Slope height, H (m)	6
Soil friction angle, ϕ ($^\circ$)	20
Soil cohesion strength, c (kPa)	18
Crack length, l_c (m)	1.5
Crack spacing, d (m)	1.0
Friction angle of crack, ϕ_c ($^\circ$)	15
Cohesion strength of crack, c_c (kPa)	0
Crack inclination, α ($^\circ$)	0
Soil unit weight, γ (kN/m ³)	18
Soil dilation angle, ψ ($^\circ$)	0
Reinforcement length, l_g (m)	2
Reinforcement strength, T (kN/m)	40
Reinforcement-soil interface coefficient, f	0.8

the slope surface (Chen et al., 2014; Mukhlisin and Khiyon, 2018; Jamalnia et al., 2020; Sari et al., 2023). So the cracks were set near the slope surface in this study.

The horizontal movement of the model was limited to the right and left sides, and no displacement was permitted at the bottom. The Reinforcement element in OptumG2 was used to model the reinforcement in the model. The mesh number could affect the accuracy of the results. Figure 3B show shows the variations of the safety factor, F of the control slope model with mesh number N . Results in Figure 3B indicate that the values of safety factor are influenced by the mesh numbers (i.e., grid density). However, F is independent on N when N is larger than 9,000. So N was set as 10,000 in this study. Besides, a mesh adaptive technique was used to help identify the slip planes (Kumar and Chauhan, 2023).

In the following sections, the parameter η is represented by the following (Eq. 6)

$$\eta = \frac{F - F_c}{F_c} \tag{6}$$

where F_c is the safety factor of the control model shown in Figure 3A.

3.1 Crack length

Figure 4 shows the variations of η with crack lengths, l_c . Results in Figure 4 indicate that: ① When the slope ratio, $\alpha = 1:1$, η decreases linearly with normalized crack length, l_c/H . However, it is important to note that the F remains larger than 1.0 within the parameters analyzed in this study, indicating that the slope is in a stable state. ② Compared with the values of η obtained when $\alpha = 1:1$, larger values of η are observed when $\alpha = 1:1.5$ and $1:2$. Additionally, unlike the linear trend observed for $\alpha = 1:1$, the calculated values of η for α

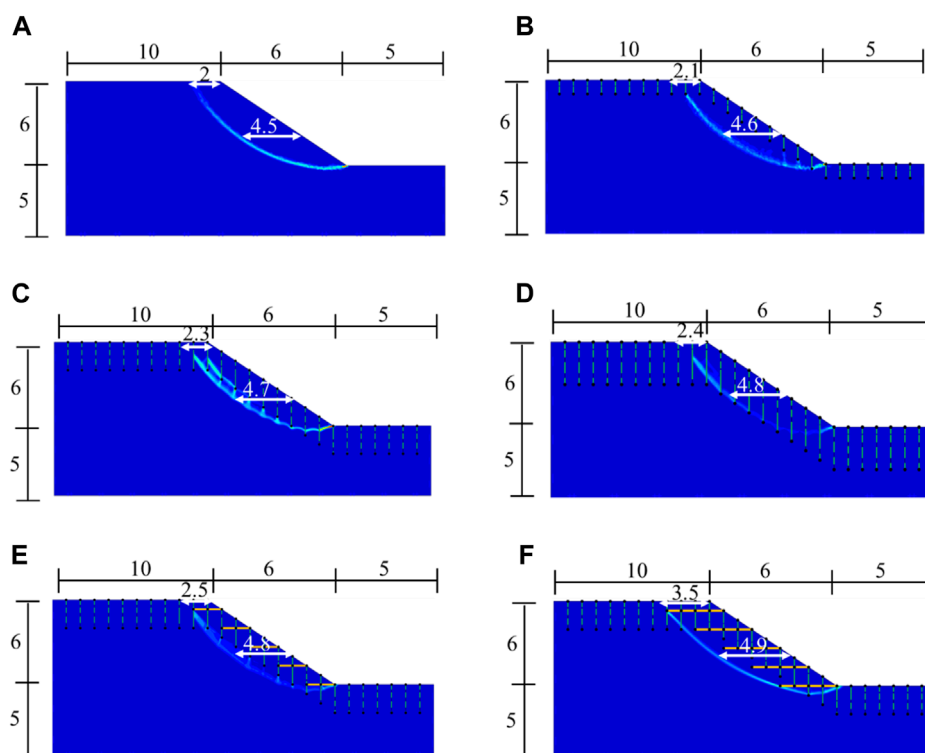


FIGURE 5 Slip planes in cases of slopes with different crack length (Unit: m): **(A)** without reinforcement ($l_g = 0$) and $l_c = 0$; **(B)** without reinforcement ($l_g = 0$) and $l_c = 1$ m; **(C)** without reinforcement ($l_g = 0$) and $l_c = 2$ m; **(D)** without reinforcement ($l_g = 0$) and $l_c = 3$ m; **(E)** with reinforcement ($l_g = 2$ m) and $l_c = 2$ m; **(F)** with reinforcement ($l_g = 4$ m) and $l_c = 2$ m.

TABLE 4 Safety factors in cases of slopes with different crack inclinations.

Inclinations		Safety factors		
		Without reinforcement ($l_g = 0$)	With reinforcement ($l_g = 2$ m)	With reinforcement ($l_g = 4$ m)
$l_c =$	$\beta = -45^\circ$	1.425	1.495	1.515
	$\beta = 0^\circ$	1.416	1.49	1.521
1 m	$\beta = 45^\circ$	1.418	1.489	1.512
$l_c =$	$\beta = -45^\circ$	1.416	1.494	1.53
	$\beta = 0^\circ$	1.304	1.429	1.499
2 m	$\beta = 45^\circ$	1.363	1.438	1.47
$l_c =$	$\beta = -45^\circ$	1.327	1.41	1.437
	$\beta = 0^\circ$	1.196	1.339	1.466
3 m	$\beta = 45^\circ$	1.303	1.369	1.404

= 1:1.5 and 1:2 initially decrease slowly with l_c/H until reaching a critical value of $l_c/H = 25\%$, beyond which a significant decreasing trend is observed. ③ The use of reinforcements enhances the stability of slopes with cracks, especially when $l_c/H > 25\%$. Furthermore,

the effectiveness of the reinforcement is greater when the crack length is larger. For example, for slopes with $l_c = 2$ m and 4 m, the safety factor can be increased by approximately 15% and 18% respectively as compared to the those without reinforcement. ④

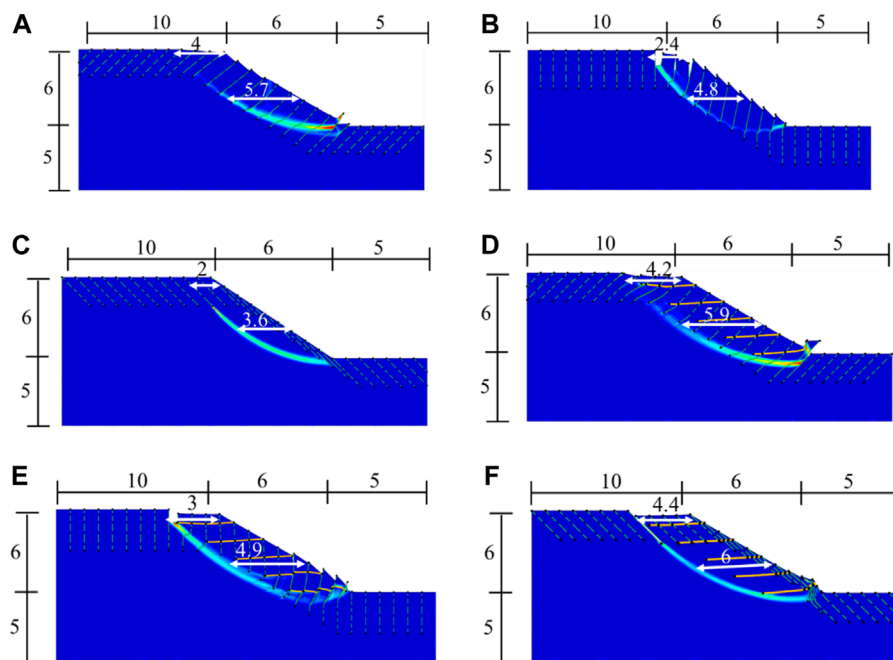


FIGURE 6 Slip planes in cases of different crack inclinations (Unit: m; crack length, $l_c = 3$ m): (A) without reinforcement ($l_g = 0$) and $\beta = -45^\circ$; (B) without reinforcement ($l_g = 0$) and $\beta = 0^\circ$; (C) without reinforcement ($l_g = 0$) and $\beta = 45^\circ$; (D) with reinforcement ($l_g = 4$ m) and $\beta = -45^\circ$; (E) with reinforcement ($l_g = 4$ m) and $\beta = 0^\circ$; (F) with reinforcement ($l_g = 4$ m) and $\beta = 45^\circ$.

Overall, the results in Figure 4 indicate that crack length have a negative impact on slope stability, especially when the slope ratio α is large.

To further analyze the reasons for the variation of the safety factor, η with crack length, l_c shown in Figure 4, Figure 5 shows the shape of slip plane for the slope with an angle ratio $\alpha = 1:1.5$ but different crack lengths, l_c . Numerous previous studies have indicated that slip planes typically originate from the slope crest

and extend downward to the slope toe (Griffiths and Marquez, 2007; Li et al., 2009; Tschuchnigg et al., 2015), which is consistent with the results shown in Figure 5. Consequently, the cracks located to the right of the slope toe (Figure 3A) have minimal impact on the stability.

Results in Figure 5 indicate than: ① The slip plane is arc-shaped when $l_c = 0$ (Figure 5A), and the exit of the slip plane is located at the toe of the slope. ② The shape of the slip plane in case of $l_c = 1$ m (Figure 5B) is almost the same as that in Figure 5A ($l_c = 0$), and there is almost no intersection between the slip plane and the crack. As a result, the corresponding values of η in Figure 2 are close to each other. ③ When the crack length, l_c increases to 2 m and 3 m (Figures 5C, D), the slip planes intersect with several cracks. Due to the lower strength of the cracks compared to the adjacent soil, the values of η in Figure 4 decrease significantly at these points. ④ Compared with the unreinforced case (Figure 5C), the slip plane is located farther away from the slope surface when reinforcements are used (Figures 5E, F), especially the reinforcement length is larger, resulting in less steep slip plane. Therefore, the corresponding values of η are relatively larger in these cases.

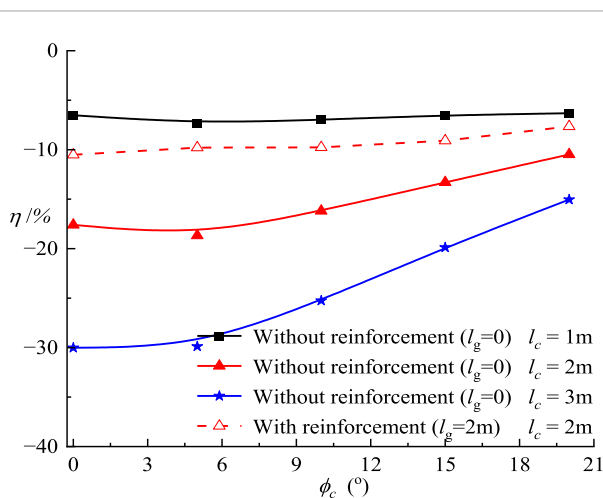


FIGURE 7 Variations of η with friction angle of cracks.

3.2 Crack inclination

The safety factors, F for slopes with different crack inclinations β , crack lengths l_c , and reinforcement lengths l_g are listed in Table 4. An inclination of $\beta = 0^\circ$ denotes a vertical crack, while $\beta = 45^\circ$ and -45° represent cracks rotating counterclockwise and clockwise, respectively, at an angle of 45° from the downward vertical line.

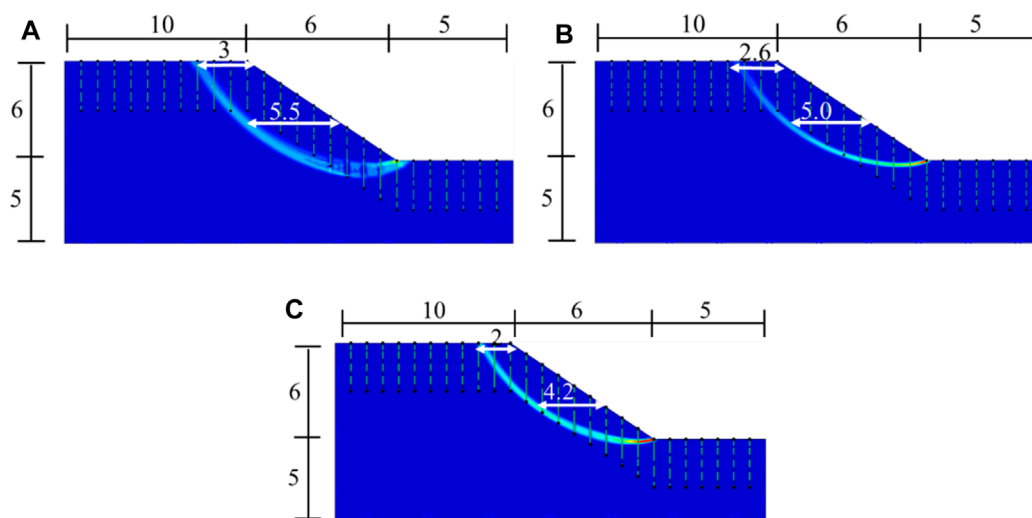


FIGURE 8
Slip planes in cases of different soil friction angle (Unit: m; $l_c = 3$ m): (A) $\phi=10^\circ$; (B) $\phi=15^\circ$; (C) $\phi=25^\circ$.

Results shown in Table 4 for slopes without reinforcement indicate that: ① When the crack length, l_c is 1 m, the inclination of the crack, β has almost no influence on the safety factor of slopes. This phenomenon may be attributed to the short length of the crack, leading to no crack intersecting with the slip plane. ② The minimum and maximum values of the safety factor, F are obtained when the crack inclination, β is 0° and -45° , respectively in the case of $l_c = 2$ m. ③ The influence of the crack inclination, β on the safety factor, F is more significant when l_c increases to 3 m as compared to those in cases of $l_c = 1$ m and 2 m.

Results shown in Table 4 also indicate that the utilization of reinforcement leads to an increase in values of the safety factor, F . Additionally, this effect is more significant for slopes with longer lengths and smaller crack inclinations.

The reasons for the variation of the safety factor, F with crack inclination, β shown in Table 4 can be explained by examining the shape of slip planes illustrated in Figure 6 for slopes with crack length $l_c = 3$ m. Results in Figure 6 indicate that: ① Cracks intersecting with the slip planes display noticeable deformation when $\beta = -45^\circ$ (Figure 6A). Although there are several inclined cracks in the slope, only relative small deformation is observed between two adjacent sliding soil masses, especially those in the middle of the slope. ② The failure mechanism of the slope is toppling collapse when the cracks are vertical ($\beta = 0^\circ$ shown in Figure 6B). Larger relative movement along the cracks is observed in this case, leading to a lower value of safety factor in Table 4. ③ The failure mechanism shown in Figure 6C is similar to that in Figure 6A, where only minimal relative deformation is observed between two adjacent sliding soil masses at the top of the slope. Besides, the slip planes overall align with the direction of the cracks, leading to a smaller value of F as compared to that in Figure 6A. ④ Compared with the failure mechanisms without reinforcement shown in Figures 6A–C, a global failure mechanism is observed in Figures 6D–F due to the reinforcement, which enhances slope integrity. The slip planes and deep cracks intersect with the reinforcement, leading to the soil masses moving together, and meanwhile, a greater value of

safety factor is obtained. Furthermore, these slip planes are located farther away from the slope surface as compared to those shown in Figures 6A–C.

3.3 Crack strength

Figure 7 shows the relationship between η and the crack friction angle, ϕ_c . Results in Figure 7 indicate that: ① Values of η for slopes without reinforcement are almost independent of the crack friction angle, ϕ_c in the case of slope with shallow cracks (i.e., $\phi_c = 1$ m). This could be attributed to the deep slip plane, leading to no intersection with cracks. ② As the crack length, l_c increases to 2 m and 3 m, η remains constant regardless of the crack strength, ϕ_c when ϕ_c is small. However, these η values show a notable increase when ϕ_c exceeds 6° . Furthermore, the influence of ϕ_c on η becomes more significant with the crack length, l_c . ③ The values of η are greater for reinforced slopes, especially when the crack strength is lower. For example, for a slope with a crack length of 2 m and crack friction angle ranging from 0 to 10° , the use of reinforcements can increase the safety factor by approximately 13%.

Figure 8 shows the shape of slip planes for slopes with different soil friction angles when the crack length is 3 m. Results in Figure 8 indicate that the soil friction angle affects the shape of the slip planes. When the soil friction angle is relatively large, the slip planes are more close to the slope surface, resulting in a smaller failure zone and a larger safety factor.

4 Conclusion

The stability of slopes with cracks was analyzed using the finite element limit analysis method. The following conclusions are drawn:

- (1) The influence of crack length on slope stability becomes more significant as the slope gradient decreases. When l_c/H exceeds

25%, a significant decrease in slope stability is observed. Using Reinforcements can increase the stability of the slope with crack, and leads to the slip planes being farther away from the slope surface. For slopes with $l_c = 2$ m and 4m, the safety factor can be increased by approximately 15% and 18% respectively as compared to the those without reinforcement.

- (2) When the crack length is relatively short, the crack inclination angle has almost no effect on slope stability. However, when the crack length is longer ($l_c/H \geq 0.33$), the slope safety factor is relatively higher for slopes with a negative crack inclination angle than that with a positive value. Reinforcement can enhance the overall integrity of the slope, improving slope stability.
- (3) Although the shape of slip planes is not influenced by the crack strength, the slope stability increases with the strength of the cracks, especially when the crack length is longer. For a slope with a crack length of 2 m and crack friction angle ranging from 0 to 10°, the use of reinforcements can increase the safety factor by approximately 13%.

5 Discussions

The finite element limit analysis method is used in this study to analyze the stability of slope with cracks. Limit analysis can be classified into two categories: upper bound analysis and lower bound analysis. The former is particularly effective in analyzing the failure mechanism of slopes (Sloan, 2013). So the upper bound limit analysis solution of slope factor are calculated using the software OptumG2. The limit analysis solutions are more rigorous than those from the traditional limit equilibrium method due to the incorporation of constitutive models and boundary conditions in the analysis. However, it should be noted that the accurate deformation cannot be obtained, which is the main shortcoming of this method.

Water plays an important role in cracked slopes. However, the software utilized in this study, OptumG2 does not incorporate the coupling of water-related processes such as rainfall infiltration and water evaporation with crack progression. So the influence of water on them can not be considered in this method.

References

- Chen, S. X., Dai, Z. J., Lu, D. J., Luo, H. M., and Li, Y. F. (2014). Stability analysis considering fracture distribution and strength for expansive soil slope. *Shuli Xuebao* 45 (12), 1442–1449. doi:10.13243/j.cnki.slx.2014.12.007
- Dick, G. J., Eberhardt, E., Cabrejo-Liévano, A. G., Stead, D., and Rose, N. D. (2015). Development of an early-warning time-of-failure analysis method-ology for open-pit mine slopes utilizing ground-based slope stability radar monitoring data. *Can. Geotech. J.* 52 (4), 515–529. doi:10.1139/cgj-2014-0028
- Gao, C. S., Xu, G. M., Zhang, L., and Yang, S. H. (2005). Centrifuge modeling of deformation and failure of slope. *Chin. J. Geotech. Eng.* 27 (4), 478–481.
- Gao, M. H., Zhang, Y. X., Wang, Z. Q., Zhao, J. Q., Sun, C., Zhou, J. M., et al. (2021). Graphic analysis method for stability of cracked slopes based on upper limit theorem. *Sci. Technol. Eng.* 21 (16), 6830–6837. doi:10.3969/j.issn.1671-1815.2021.16.043
- Griffiths, D. V., and Marquez, R. M. (2007). Three-dimensional slope stability analysis by elasto-plastic finite elements. *Géotechnique* 57 (6), 537–546. doi:10.1680/geot.2007.57.6.537
- Jamalinia, E., Vardon, P. J., and Steele-Dunne, S. C. (2020). The impact of evaporation induced cracks and precipitation on temporal slope stability. *Comput. Geotech.* 122, 103506. doi:10.1016/j.compgeo.2020.103506
- Krabbenhoft, K., Lyamin, A., and Krabbenhoft, J. (2015). Opium computational engineering (OptumG2). *Comput. Softw.*
- Kumar, P., and Chauhan, V. B. (2023). On the eccentrically loaded strip footing resting over a circular cavity in the rock mass: adaptive finite-element analysis, observations, and recommendations. *Int. J. Geomech.* 23 (2), 04022287. doi:10.1061/ijgnai.gmng-7985

Data availability statement

The raw data supporting the conclusion of this article will be made available by the authors, without undue reservation.

Author contributions

CH: Conceptualization, Formal Analysis, Investigation, Methodology, Writing–original draft. Y-HZ: Supervision, Writing–original draft, Writing–review and editing. H-YY: Formal Analysis, Software, Validation, Writing–original draft.

Funding

The author(s) declare financial support was received for the research, authorship, and/or publication of this article. This research was funded by Key R&D Program of Shandong Province (Grant No. 2020CXGC010310).

Acknowledgments

The authors are grateful to reviewers for their helpful comments and suggestions.

Conflict of interest

Authors CH, Y-HZ, and H-YY were employed by China Railway Eryuan Engineering Group Co., Ltd.

Publisher's note

All claims expressed in this article are solely those of the authors and do not necessarily represent those of their affiliated organizations, or those of the publisher, the editors and the reviewers. Any product that may be evaluated in this article, or claim that may be made by its manufacturer, is not guaranteed or endorsed by the publisher.

- Li, L. C., Tang, C. A., Zhu, W. C., and Liang, Z. Z. (2009). Numerical analysis of slope stability based on the gravity increase method. *Comput. Geotech.* 36 (7), 1246–1258. doi:10.1016/j.compgeo.2009.06.004
- Lin, P., Liu, X., Zhou, W., Wang, R., and Wang, S. (2015). Cracking, stability and slope reinforcement analysis relating to the Jinping dam based on a geomechanical model test. *Arab. J. Geosci.* 8, 4393–4410. doi:10.1007/s12517-014-1529-1
- Mehrjardi, G. T., Ghanbari, A., and Mehdizadeh, H. (2016). Experimental study on the behaviour of geogrid-reinforced slopes with respect to aggregate size. *Geotext. Geomembranes* 44 (6), 862–871. doi:10.1016/j.geotextmem.2016.06.006
- Mukhlisin, M., and Khiyon, K. N. (2018). The effects of cracking on slope stability. *J. Geol. Soc. India* 91, 704–710. doi:10.1007/s12594-018-0927-5
- Sari, P. T. K., Mochtar, I. B., and Chaiyaput, S. (2023). Effectiveness of horizontal sub-drain for slope stability on crack soil using numerical model. *Geotech. Geol. Eng.* 41 (8), 4821–4844. doi:10.1007/s10706-023-02550-1
- Sloan, S. W. (2013). Geotechnical stability analysis. *Géotechnique* 63 (7), 531–571. doi:10.1680/geot.12.RL.001
- Stockton, E., Leshchinsky, B. A., Olsen, M. J., and Evans, T. M. (2019). Influence of both anisotropic friction and cohesion on the formation of tension cracks and stability of slopes. *Eng. Geol.* 249, 31–44. doi:10.1016/j.enggeo.2018.12.016
- Tschuchnigg, F., Schweiger, H. F., Sloan, S. W., Lyamin, A. V., and Raissakis, I. (2015). Comparison of finite-element limit analysis and strength reduction techniques. *Géotechnique* 65 (4), 249–257. doi:10.1680/geot.14.P.022
- Xu, P., Jing, G. L., Qiu, J. J., Lin, Z. Z., and Wang, Z. M. (2018). Limit analysis on yield acceleration and failure model of reinforced soil retaining walls using two-wedge method. *Rock Soil Mech.* 39 (8), 2765–2770. doi:10.16285/j.rsm.2016.2419
- Xu, P., Li, T., and Hatami, K. (2020). Limit analysis of bearing capacity and failure geometry of GRS bridge abutments. *Comput. Geotech.* 127, 103758. doi:10.1016/j.compgeo.2020.103758
- Yin, Y., Deng, Q., Li, W., He, K., Wang, Z., Li, H., et al. (2023). Insight into the crack characteristics and mechanisms of retrogressive slope failures: a large-scale model test. *Eng. Geol.* 327, 107360. doi:10.1016/j.enggeo.2023.107360
- Zhang, G., Hu, Y., and Zhang, J. M. (2009). New image analysis-based displacement-measurement system for geotechnical centrifuge modeling tests. *Meas* 42 (1), 87–96. doi:10.1016/j.measurement.2008.04.002
- Zhang, W. W. (2022). Study on evaluation method of rainfall erosion and maintenance scheme for embankment slope of heavy haul railway in UAD desert area. *Railw. Constr. Technol.* 05, 95–98.
- Zhou, Z., Zhang, J., Ning, F., Luo, Y., Chong, L., and Sun, K. (2020). Large-scale test model of the progressive deformation and failure of cracked soil slopes. *J. Earth. Sci.* 31, 1097–1108. doi:10.1007/s12583-020-1342-6